Title:

Pressure Response during Filtration and Oxidation in Diesel Particulate Filter

Authors:

Kazuhiro YAMAMOTO [1], Hiroya KATO [1], Daisuke SUZUKI [1]

[1] Department of Mechanical System Engineering, Nagoya University

Correspondence:

Kazuhiro YAMAMOTO

Furo-cho, Chikusa-ku, Nagoya-shi, Aichi 464-8603, JAPAN

Tel: +81-52-789-4471 E-mail: kazuhiro@mech.nagoya-u.ac.jp

Abstract:

Combustion-generated soot particles that arise from diesel vehicles are known to cause substantial damages to the environment as well as to human health. A diesel particulate filter (DPF) is needed to trap nanoparticles in the diesel exhaust after-treatment. In the present study, using carbon particles as model soot, we evaluated the filtration and regeneration performances of diesel or gasoline soot in SiC-DPF. Especially, particles with different size distributions were used. Results show that, independent of the particle size, the pressure drop raised by the particle deposition almost exhibits the same dependence on the deposited particle mass. When the volumetric flow rate is increased, the smaller particle can pass through the filter but the larger particle is trapped more efficiently. In the filter regeneration process, CO and CO_2 concentrations initially increase with the lapse of time, reach the maximum, and then decrease gradually. The decreasing rate in the pressure drop is the largest in Case 3 of the smallest particle distribution, followed in order by Cases 2 and 1. Since the particle density in Case 3 is the lowest, it is derived that the sparse deposition layer composing of smaller particles is oxidized more easily, resulting in the shorter period of the filter regeneration. By comparing the variation of the pressure drop during the filtration and the regeneration, the dependence of the pressure drop on the deposited particle mass is different, showing the hysteresis in the transition of the pressure drop.

Keywords:
Diesel particulate filter; Filtration; Diesel soot; Pressure drop, Particle size

1 Introduction

It is well-known that combustion-generated soot particles that arise from vehicles and factories are known to cause substantial damages to the environment as well as to human health [1]. Compared with ordinary gasoline engines, diesel engines emit significant amounts of particulates. Most of diesel soot exists in the so-called accumulation mode in the 100−300 nm diameter range, and the nuclei mode of typically consists of particles in the 5-50 nm diameter range. The nuclei mode contains 1−20% of total particle mass and more than 90% of total particle number [2]. Following aspiration, nanoparticles deposit onto the alveoli in the deepest parts of the lung, and then penetrate the cell wall, allowing entry into the blood stream and other organs. Since the long-term particle aspiration is reported to raise carcinogenicity, regulations for the particle emission continue to be tightened worldwide, year-by-year. For example, the EU has set the Euro VI regulations for the particle number (PN) as well as the conventional particle weight (particle mass, PM) [3,4]. Based on the above, modern diesel vehicles are forced to equip with a diesel particulate filter (DPF) in the exhaust after-treatment system.

Nowadays, the share of gasoline direct injection (GDI) engines with better fuel economy has been increasing. Hereafter, we need to handle particle emissions even from gasoline vehicles, because GDI engines emit considerably more particles compared with conventional port fuel injection (PFI) engines. It is worth noting that the particle size from GDI engines is significantly smaller than that of diesel soot. Accordingly, the recent European regulation includes the emission limit of gasoline soot, as well. To control the particle emissions from gasoline vehicles, we now need a gasoline particulate filter (GPF) [5]. The most challenging task is to provide the sufficient particle number reduction at acceptable filter backpressure, in order not to compromise the CO_2 advantage of GDI engines [6].

As in the case of DPF, GPF would be clogged by collected particles with a rise of the filter backpressure (pressure drop across the filter), resulting in

subsequent worsening of fuel efficiency and a decrease in the engine output. For this reason, a filter regeneration process is required, by which an incineration step is conducted to oxidize and remove deposited particles [7-9]. To improve the filtration efficiency together with the reduction of the pressure drop, we need to know the regeneration performance as well. So far, it is difficult to discuss the phenomena of filtration and oxidation processes inside the filter, because the characteristics of emitted particles depend on fuel properties, the exhaust gas component, and engine conditions [10-12]. In the literatures, as model soot, commercial carbon black such as Printex-U was used [10,13-15], but it was tough to add solid particles uniformly in the flow of the mimic exhaust gas. Alternatively, the soot originated from the burner may be used, but the effect of non-oxidative/evaporative components could arise [16,17].

In the present study, focusing on non-volatile soot particles in the vehicle exhaust, we used carbon particles produced by a carbon particle generator [18]. Based on the size distribution of typical gasoline and diesel soot [19-21], we determined the experimental conditions. Currently, it is difficult to get GPF in the market, but it is reported that the porous structure of GPF is similar to that of DPF [5]. Then, we investigated the filtration and oxidation processes of SiC-DPF. By considering the smaller particles, we collected some fundamental knowledge for the product specification of GPF. The oxidation of carbon particles were analyzed by monitoring the particle number concentration, together with the measurement of CO and CO_2 concentrations.

2 Experimental Setup

2.1 Particle Trap in Filtration Test

We examined the filtration performance in terms of the filtration efficiency and the pressure drop. Here, we explain an experimental setup for filtration of carbon particles. Figure 1 shows a schematic diagram of the filtration test. In experiments, we used the carbon particle generator (DNP-2000; Palas GmbH, Germany). It can emit particles having a fixed size distribution, suitable for laboratory experiments [18]. The principle involves the use of two highly purified graphite rods as electrodes with a discharge of 3000 V to generate nanoparticles. The particle concentration was controlled by changing the discharge voltage. The

different particle size distributions were formed, simulating gasoline or diesel soot [19-21]. Since the carbon particle generator showed a good repeatability, it was appropriate to discuss the effect of the size distribution on the filtration performance.

In the filtration test, nitrogen was used as carrier gas, and carbon particles were uniformly added to the flow. A small size of DPF in Fig. 2 was inserted into a silica tube installed through a tubular furnace. The DPF was placed inside the furnace in the flow path, and carbon particles were trapped by the filter. The SiC-DPF was the monolithic wall-flow type filter, with a diameter of 26 mm and a length of 20 mm. Its cell density was 300 cpsi, its wall thickness was 0.25 mm, its porosity was 42%, and its average pore size was 11 μm. These were typical values of the honeycomb DPF [20,21].

Next, we explain experimental conditions. In the filtration test, the flow was fed at room temperature (25°C) through the quartz tube where the filter was installed. The feeding of the volumetric flow rate was changed from 4 to 40.4 L/min, corresponding to the inflow velocity of 12.6 to 127 cm/s. When we intended to supply carbon particles at high temperature, the volumetric flow rate was raised to keep the constant feeding rate of particles at the different temperature. In this case, the increased volumetric flow rate compensated the reduction of the flow density. The size and the number concentration of carbon particles, which were sampled from the gas after passing through the filter, were measured using a scanning mobility particle sizer (SMPS, Model-3034D; TSI Inc., USA). The sampling period was 3 min. To inhibit particles from being agglomerated during sampling, the particles were diluted 100 times using an automobile exhaust gas dilution device (MD19-3E; Matter Engineering AG, Switzerland) [18].

Figure 3 shows the size distribution of carbon particles used in experiments. Three different size distributions were considered. The condition of the maximum concentration capable of the carbon particle generator was Case 1, where the peak diameter in the size distribution was 111 nm. In Case 2, the peak diameter was 72 nm. To consider the mimic gasoline particulate, the peak diameter was set to be 47 nm in Case 3. The total number concentrations in three cases were 2.06×10^7, 1.55×10^7, 8.10×10^6, respectively. The mass of carbon particles deposited in the DPF, m, was obtained by the direct weight measurement with an electronic

balance. By assuming the sphere of the carbon particle, these particle densities of Cases 1 to 3 were 1030, 813, and 646 kg/m^3.

The pressure drop of ΔP was measured using two pressure sensors (VHR3; VALCOM Co., Ltd., Japan). One was for monitoring the filter backpressure, and the other was for the atmospheric pressure. The filtration efficiency f_N was calculated using formula 1, which was based on the number concentration:

$$f_N = \frac{\sum N_0(d_i) - \sum N(d_i)}{\sum N_0(d_i)} \qquad (1)$$

where d_i represents each particle size classified by SMPS, N_0 (d_i) presents the number of carbon particles with a particle size of d_i before the filter, and N(d_i) presents the number of carbon particles after the filter. We set the filtration period to be 30 min in Case 1. At this time, the final value of the pressure drop in Case 1 was 0.308 kPa. On the other hand, as seen in profiles in Fig. 3, the particle number concentrations in Cases 2 and 3 were lower, and we continued the filtration test until the pressure drop reached 0.308 kPa. Resultantly, the filtration periods in Cases 2 and 3 were 110 min and 650 min, respectively.

2.2 Carbon Particle Oxidation in Filter Regeneration Test

To realize the carbon oxidation at fixed temperature, an electric tubular furnace (ARF-30MC; Asahi Rika Seisakusho Co. Ltd., Japan) was used [18]. The furnace size was 186 × 300 mm, equipped with a digital temperature controller (AMF-S, Asahi Rika Seisakusho Co. Ltd., Japan). It is possible to heat the flow up to 1200 ºC with a temperature adjustment error of ± 2.5 ºC. In experiments, by using two thermocouples, we adjusted the furnace temperature so that the DPF inlet temperature was set to be constant [22]. It should be noted that, for keeping the same condition in the filter regeneration test, the DPF inlet temperature was a favorable parameter. Instead, the DPF outlet temperature was inappropriate, because the temperature would be inevitably increased due to the oxidation of carbon particles.

Let us explain the experiment procedure in the filter regeneration test. First, carbon particles were trapped by DPF until the pressure drop in Cases 1 to 3 exhibited the same value. If not specified explicitly, the temperature during the

filtration is room temperature. When we intended to oxidize the carbon particles deposited in DPF, a mixture of oxygen and nitrogen was flowed at the higher temperature. Similar to the filtration test, the pressure drop was monitored. At the same time, the burned gas after passing through the DPF was sampled, and the concentrations of CO and CO_2 were measured using an infrared gas analyzer (CGT-7000; Shimadzu Corporation, Japan).

In the filter regeneration test, the DPF inlet temperature was 550 °C [20]. The composition of the flow was 10% oxygen and 90% nitrogen. The filter regeneration test was continued until the pressure drop became the value before the carbon particle deposition. It corresponded to the initial pressure drop at 550 °C, ensuring that all deposited particles were oxidized.

3 Results and Discussion

3.1 Filtration Performance and Pressure Drop

First, the filtration tests in Cases 1 to 3 were conducted. Figure 4 shows the temporal changes in the filtration efficiency and the pressure drop. The time of *t* was counted when we started the particle feeding. The volumetric flow rate was 4.0 L/min. Each test was continued when the pressure drop reached the same value of 0.308 kPa. As shown in this figure, both the filtration efficiency and the pressure drop increase with time. For all cases, after the filtration efficiency becomes nearly 100%, the pressure drop linearly increases, which is similar to the experiments of the real diesel soot [20-23]. The times when the filtration efficiency was close to 100% in Cases 1–3 were approximately 6, 18, and 65 min, respectively. Before that, the leakage of carbon particles through the filter was confirmed. The above tendencies are the well-known phenomenon when the depth filtration, in which particles are deposited inside the filter walls, shifts to the surface filtration, in which particles are deposited on the filter wall surface. Figure 5 shows the relationship between the pressure drop and the mass of deposited particles in DPF, *m*. In this case, the volumetric flow rate was also 4.0 L/min. As shown in this figure, the relationship in Cases 1 to 3 almost exhibits the same curve. In other words, independent of the particle size, the same pressure drop would be observed if the mass of deposited particles is equal. In this experiment, only carbon particles were used. Any soluble organic fraction (SOF), water vapor

and the gas component of hydrocarbons were not included in the flow. Then, less dependence of the pressure drop on the particle size could appear.

Next, the volumetric flow rate was changed. Figure 6 shows the temporal changes in the filtration efficiency and the pressure drop. The volumetric flow rate was varied from 4.0 to 40.4 L/min. The feeding of the particles in Case 2 was applied. For all cases, the filtration efficiency reaches close to 100%. As the volumetric flow rate increases, the pressure drop monotonically increases. This is because the pressure drop is simply proportional to the flow rate. For further study, the filtration efficiency for each particle size at t = 3 min is compared in Fig. 7. It is seen that the filtration efficiency apparently depends on the particle size. When the flow rate is increased, smaller particles can pass through the filter but larger particles are trapped more efficiently.

It is reported that, in a fresh DPF, the main trapping mechanism composes of the Brownian diffusion and the interception effect [10,20,23]. The smaller particles preferentially deposit on the filter surface due to the Brownian motion. The interception on the filter substrate largely depends on the filtration velocity. When the flow rate is increased, the corresponding filtration velocity is higher. Resultantly, the trapping by the Brownian motion would be relatively reduced at higher flow rate. That is why the filtration efficiency of the smaller particle is worsened when the flow rate is increased in Fig. 7.

3.2 Particle Oxidation during Filter Regeneration

Next, the effects of the particle size on the filter regeneration were investigated. Each DPF in which carbon particles in Cases 1 to 3 had been deposited in advance were regenerated by the tubular furnace. The pressure drop and the concentrations of CO and CO_2 were monitored. As found in Fig. 5, when the mass of deposited particles in DPF is the same, the pressure drop shows the same value. Then, we regenerated three filters in which the same amount of particles was deposited. These pressure drops were shown by dotted line in Fig. 5. As already mentioned, the DPF inlet temperature was set to be 550 °C. Results are shown in Fig. 8. In this figure, ΔP_{550} represents the final pressure drop when all particles are oxidized at 550°C. When the pressure drop was equal to this value, the filter regeneration process was judged to be completed. For all cases, the pressure drop monotonically decreases with time. However, the decreasing rate of

the pressure drop in Case 3 is the largest, followed in order by Cases 2 and 1. As explained in section 2.1, the particle density in Case 3 was the lowest. Therefore, it is suggested that the sparse deposition layer composing of smaller particles is oxidized more easily.

To confirm the above explanation, the emissions of CO and CO_2 produced in the carbon oxidation process were measured. Results are shown in Fig. 9, which are the sum of CO and CO_2 volume fractions in the flow. It is seen that, for all cases, CO and CO_2 concentrations initially increased with time, took the maximum approximately 10 s after we started the regeneration test, and decreased gradually. Interestingly, in Case 3, more CO and CO_2 were produced, and then, these concentrations decayed more quickly. It should be noted that, in Case 3, the decreasing rate of the pressure drop in Fig. 8 is larger than other two cases. Again, it is emphasized that the sparse deposition layer in Case 3 is formed. Previous work [24] has reported that, in the case of the smaller diesel soot, the porosity of soot deposition layer is larger. Since there are more pores between deposited particles, it is easier to supply the oxygen in the sparse deposition layer. It is concluded that, as the smaller particles are deposited, the period of the filter regeneration can be shortened.

3.3 Consecutive Filtration and Oxidation Test

Finally, the consecutive filtration and oxidation (filter regeneration) test was conducted. That is, after the filtration test was finished at high temperature, the filter regeneration was immediately started at the same temperature, mainly in order to observe the different response of the pressure drop in filtration and regeneration processes. In this test, the DPF inlet temperature was always kept at 550°C. The carbon particles in Case 1 were used. To avoid the oxidation of particles during the filtration, only nitrogen was fed at the flow rate of 4.0 L/min. Subsequently, during the filter regeneration, nitrogen and oxygen were supplied at the flow rates of 3.6 and 0.4 L/min, respectively. The filtration test was performed for 30 minutes, and the regeneration test was continued until the pressure drop decreased to ΔP_{550} where all carbon particles were oxidized.

Figure 10 shows the obtained temporal change in the pressure drop. As shown in this figure, the pressure drop draws a convex curve during the filtration, and conversely a concave curve during the filter regeneration. As a result, the time

response of the pressure drop is found to be different in filtration and regeneration processes. It should be noted that, the deposition rate of particles during the filtration was nearly constant due to the fixed feeding of particles. On the other hand, the oxidation rate of particles was expected to be changed even when the temperature was constant, because the oxidation of carbon particles was passive process in which the reaction rate was accordingly varied when both of carbon particles and oxygen were consumed. Therefore, the pressure drop was re-examined as a function of the mass of deposited (or remained) carbon particles inside the filter. Since the filter could not be detached during the filter regeneration, the mass of carbon particles remained inside the filter was estimated from the total emissions of CO and CO_2. It was described by (m_0 - m_b), where m_0 (= 0.0025 g) was the initial mass of carbon particles right after the filtration, and m_b is the mass of oxidized carbon particles.

Figure 11 shows the relationship between the mass of carbon particles and the pressure drop during the filtration or the oxidation of carbon particles, which is obtained by re-plotting Fig. 10. Clearly, in filtration and regeneration processes, the value of the pressure drop is different even when each deposited particle mass is the same. To explain the different response in the pressure drop, we focus on the area where the particles are deposited. We need to think of the shift between the depth filtration and the surface filtration during the filtration [10,12,21]. That is, the area of particle deposition moves from the inner part to the surface part of the filter. However, in the case of the filter regeneration, the oxidation of carbon particles occurs everywhere in the filter, because the oxygen in the flow is transported deeply into the sparse deposition layer of particles. Hence, in the filtration and regeneration processes, even though the mass of deposited particles is the same, the spatial distribution of carbon particles could be different. Consequently, the hysteresis in the transition of the pressure is observed. Although, depending on regeneration conditions and soot type, more wide range of soot size may appear in the real situation, this information is indispensable in predicting the filter regeneration rate based on the pressure drop.

4 Conclusions

In the present experiments, carbon particles and SiC-DPF were used to simulate the filtration and regeneration processes of diesel or gasoline soot. Three

different particle size distributions were tested. The results are summarized as follows:

(1) Independent of the particle size distribution, the filtration efficiency and the pressure drop increase with time. When the depth filtration is shifted to the surface filtration, the filtration efficiency reaches close to 100% and the linear pressure rise is observed. When the volumetric flow rate is constant, the relationship between the pressure drop and the mass of deposited particles in the filter almost exhibits the same curve. When the volumetric flow rate is increased, the pressure drop becomes larger. In this case, the smaller particle can pass through the filter but the larger particle is trapped more efficiently.

(2) As for the filter regeneration process, regardless of the size distribution of oxidized carbon particles, CO and CO_2 concentrations initially increase with time, takes the maximum approximately 10 s after starting the regeneration, and then decrease gradually. The decreasing rate of the pressure drop is the largest in Case 3, followed in order by Cases 2 and 1. Since the particle density in Case 3 is the lowest, the sparse deposition layer composing of smaller particles is oxidized more easily, resulting in the shorter period of the filter regeneration.

(3) Based on the results in consecutive filtration and oxidation of particles at high temperature, the pressure drop shows a convex curve during filtration and a concave curve during regeneration. This is because the oxidation rate of carbon particles would be changed even at the constant temperature due to the passive oxidation process. Moreover, in filtration and regeneration processes, the different pressure drop is observed even though the mass of deposited particles is the same, showing the hysteresis in the transition of the pressure drop.

Acknowledgments

This work was partially supported by The Research association of Automotive Internal Combustion Engines (AICE) in Japan.

References

1. Kennedy, I. M.: Proc. Combust. Inst. 31, 2757-2770 (2007).
2. Kittelson, D. B.: J. Aerosol Science 29, 575-588 (1998).

3. Official Journal of the European Union, Regulation (EC) No. 595/2009, July 18 (2009).
4. Johnson, T. V.: SAE Technical Paper 2010-01-0301, 16-29 (2010).
5. Ito, Y., Shimoda, T., Aoki, T., Shibagaki, Y., Yuuki, K., Sakamoto, H., Vogt, C., Matsumoto, T., Heuss, W., Kattouah, P., Makino, M., Kato, K.: SAE Technical Paper 2013-01-0836, 1-10 (2013).
6. Spiess, S., Wong, K. F., Richter, J. M., Klingmann, R.: Top Catal 56, 434-439 (2013).
7. Koltsakis, G. C., Stamatelos, A. M.: Prog. Energy Combust. Sci. 23, 1-39 (1997).
8. Park, D. S., Kim, J. U., Kim, E. S.: Combust. Flame 114, 585-590 (1998).
9. Kimura, M., Muramatsu, T., Kunishima, E., Namima, J., Crawley, W., Parrish, T.: SAE technical paper 2011-01-0295, 9-17 (2011).
10. Yamamoto, K., Nakamura, M.: ASME J. Heat Transfer, 133, No.6, 1-10 (2011).
11. Yamamoto, K., Nakamura, M., Yane, H., Yamashita, H.: Catalysis Today, 153, 118-124 (2010).
12. Yamamoto, K., Yamauchi, K.: Proc. Combust. Inst., 34, 3083-3090 (2013).
13. Setiabudi, A., van Setten, B. A.A.L., Makkee, M., Moulijn, J. A.: Applied Catalysis B, 35, 159-166 (2002).
14. Setiabudi, A., Makkee, M., Moulijn, J. A.: Applied Catalysis B, 50, 185-194 (2004).
15. Jeguirim, M., Tschamber, V., Brilhac, J. F.: J. Chem. Technol. Biotechnol. 84, 770-776 (2009).
16. Shrivastava, M., Nguyen, A., Zheng, Z. Q., Wu, H. W., Jung, H. S.: Environ. Sci. Tech. 44, 4796-4801 (2010).
17. Lizarraga, L., Souentie, S., Boreave, A., George, C., D'Anna, B., Vernoux, P.: Environmental Sci. Tech. 45, 10591-10597 (2011).
18. Yamamoto, K., Kanamori, Y.: SAE Technical Paper 2015-01-1995, 1-7 (2015).
19. Su, D. S., Jentoft, R. E., Müller, J-O., Rothe, D., Jacob, E., Simpson, C. D., Tomović, Ž., Müllen, K., Messerer, A., Pöschl, U., Niessner, R., Schlögl, R.: Catalysis Today 90, 127 -132 (2004).

20. Tsuneyoshi, K., Takagi, O., Yamamoto, K.: SAE Technical Paper 2011-01-0817, 297-305 (2011).
21. Tsuneyoshi, K., Yamamoto, K.: Energy, 48, 492-499 (2012).
22. Tian, Z. Y., Bahlawane, N., Vannier, V., Kohse-Höinghaus K.: Proc. Combust. Inst. 34, 2261-2268 (2013).
23. Wirojsakunchai, E., Schroeder, E., Kolodziej, C., Foster, D. E., Schmidt, N., Root, T., Kawai, T., Suga, T., Nevius, T., and Kusaka, T.: SAE Technical Paper 2007-01-0320 (2007).
24. Konstandopoulos. A. G, Skaperdas.E.: SAE paper 2002-01-1015 (2002).

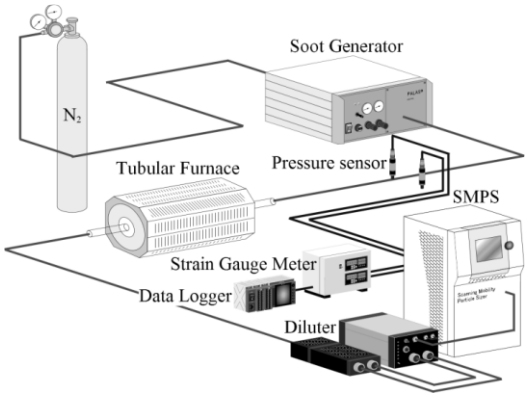

Fig. 1 Experimental setup for particle filtration test.

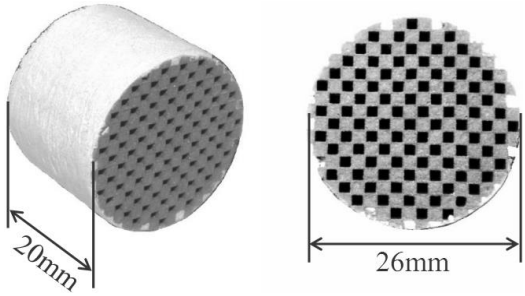

Fig. 2 Picture of SiC-DPF

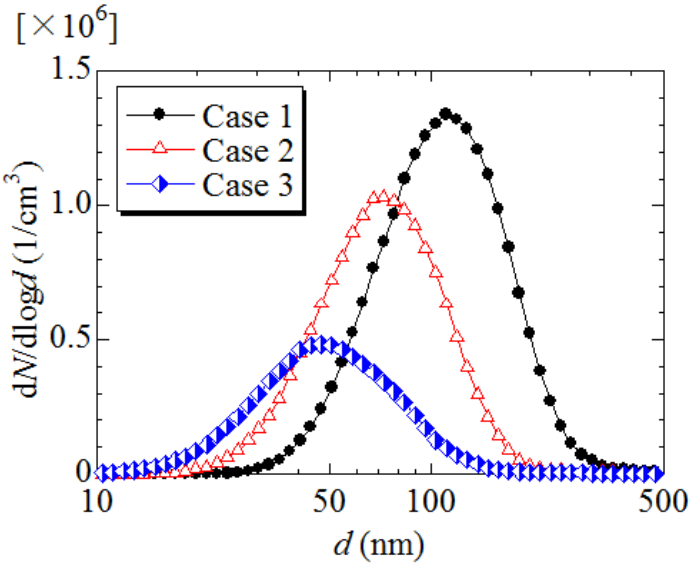

Fig. 3 Particle size distribution.

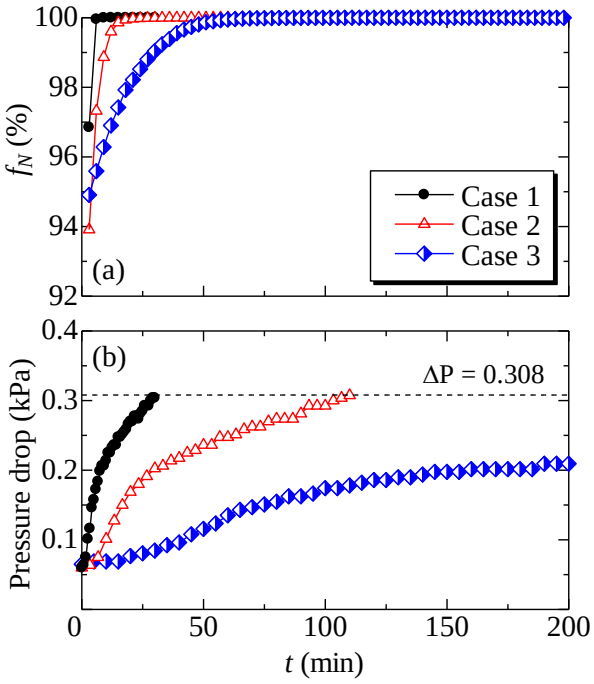

Fig. 4 Temporal changes in (a) filtration efficiency and (b) pressure drop.

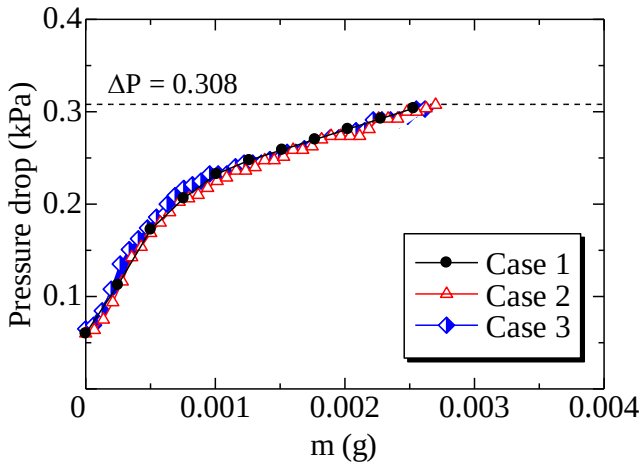

Fig. 5 Relationship between mass of deposited particles and pressure drop.

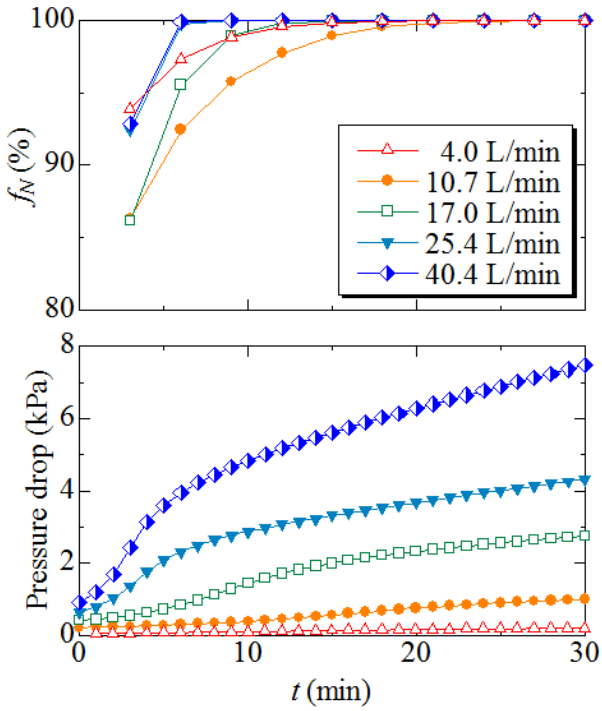

Fig. 6 (a) Filtration efficiency and (b) pressure drop in Case 2.

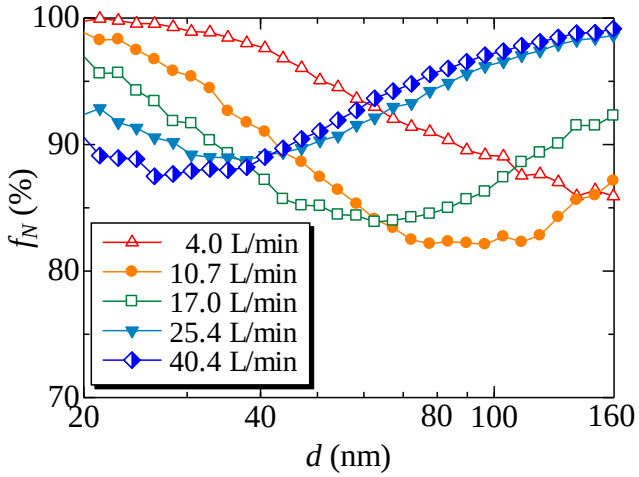

Fig. 7 Filtration efficiency for each particle size at t = 3 min by changing the flow rate in Case 2.

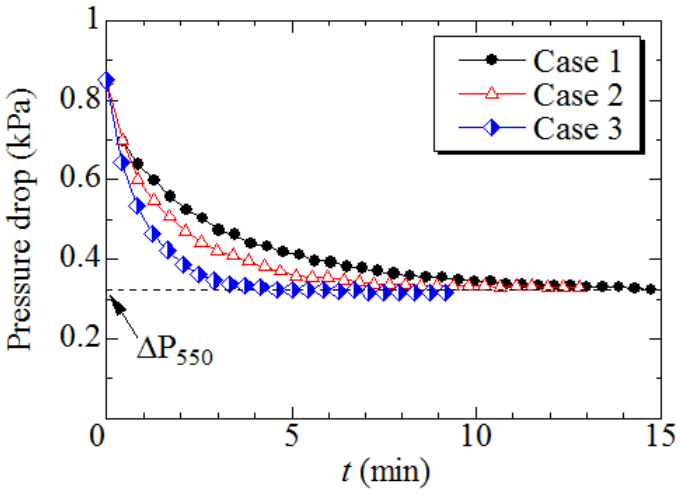

Fig. 8 Pressure drop in filter regeneration test.

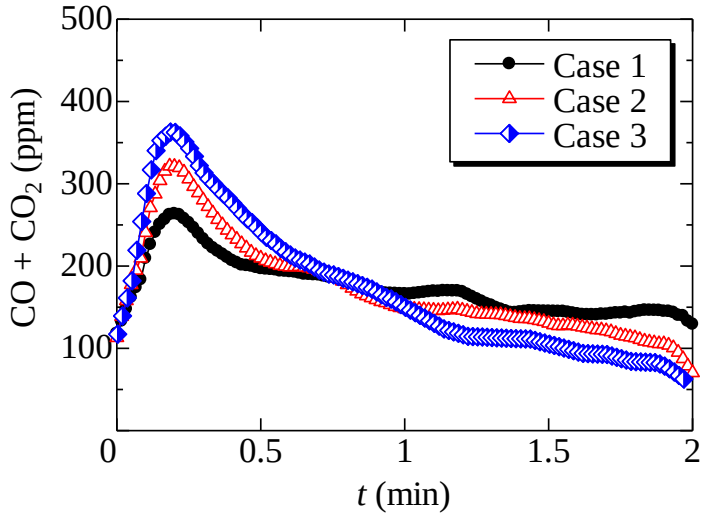

Fig. 9 Volume fraction of CO and CO_2.

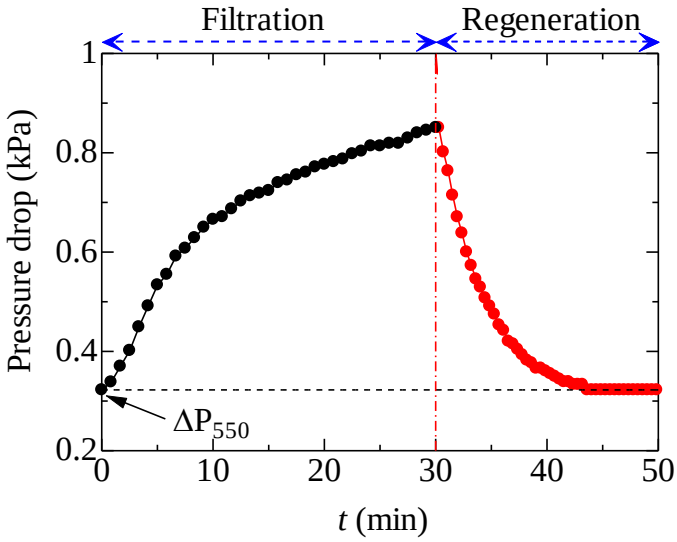

Fig. 10 Temporal change in pressure drop in Case 1 in consecutive filtration and oxidation test.

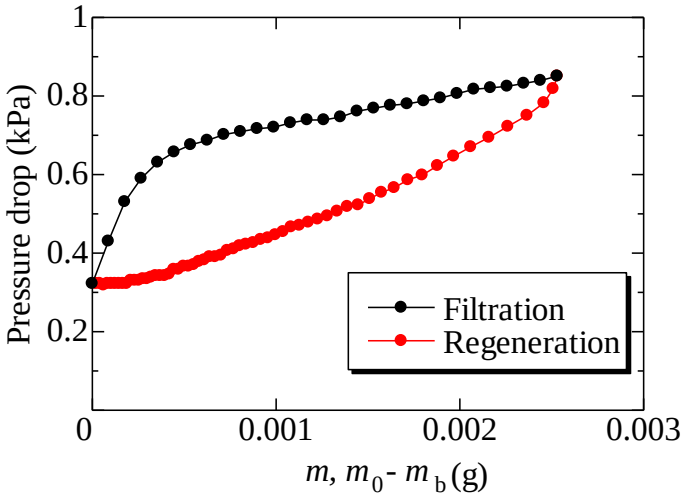

Fig. 11 Relationship between mass of carbon particles and pressure drop during filtration and regeneration.